



ILJS-24-094 (SPECIAL EDITION)

2-D Spectral Analysis of Aeromagnetic Anomalies over Parts of Bida Basin, Nigeria

Issa T. A.,¹ Olatunji S.² and *Omolaiye G. E.².

¹ Department of Geology and Mineral Science, Kwara State University, Malete

² Department of Geophysics, University of Ilorin, PMB 1515, Ilorin, Nigeria

Abstract

The average depth of magnetic sources was estimated in some portions of the Bida Basin. A 2-D spectral analysis of aeromagnetic anomalies over six aeromagnetic map sheets, each spanning an area of $\frac{1}{2}^\circ \times \frac{1}{2}^\circ$ on a scale of 1:100,000, was carried out. To identify residual features and draw attention to the more intense anomalies in comparison to the strong regional gradients, data augmentation techniques were used. Adopted techniques include various filtering approaches, trend surface analysis, and computations reducing to the equator. The result shows the two-depth source model of the part of the basin with an average depth of the deeper magnetic sources at 3.26 km, which corresponded to the magnetic basement surface. This layer may be associated with intra-basement characteristics including faults and fractures, lateral changes in basement susceptibilities, and magnetic rocks found in the basement. There are magnetic intrusive bodies within the sediments, as evidenced by the average depth of 1.22 km and a range of 0.68 km to 2.32 km for the shallower magnetic sources. The magnetic source's average depth of 3.26 km to the basement indicates a sufficient sedimentary thickness for potential hydrocarbon accumulation. The undulating nature of the basement surface may create traps for hydrocarbons, suggesting that the possibility of hydrocarbon accumulation cannot be ruled out.

Keywords: Bida Basin, Spectral Analysis, Magnetic Source, Aeromagnetic Sheets, 2-D spectral analysis

1.0 INTRODUCTION

An essential technique for estimating the basement depth beneath the sedimentary cover is the examination of aeromagnetic data. The earth's surface is home to a wealth of valuable resources, including groundwater, oil, gas, and economic minerals. Geophysical studies of subsurface structures can be used to assess the presence and volume of these resources. Scientists can find vertical and lateral changes in the interior of the earth by evaluating and interpreting geophysical measurements, which can provide important insights into the geological formations below the surface.

The study area is part of Bida Basin and is constrained by Latitudes $8^{\circ}30'$ to $9^{\circ}30'$ N and Longitudes 5° to $6^{\circ}30'$ E situated in the west of central Nigeria (Fig. 1). This study area covers Mokwa, Egbako, Bida, Lafigi, Pategi, and Baro sheets.

Corresponding Author: Omolaiye G. E.

Email: gab_omolaiye@yahoo.co.uk

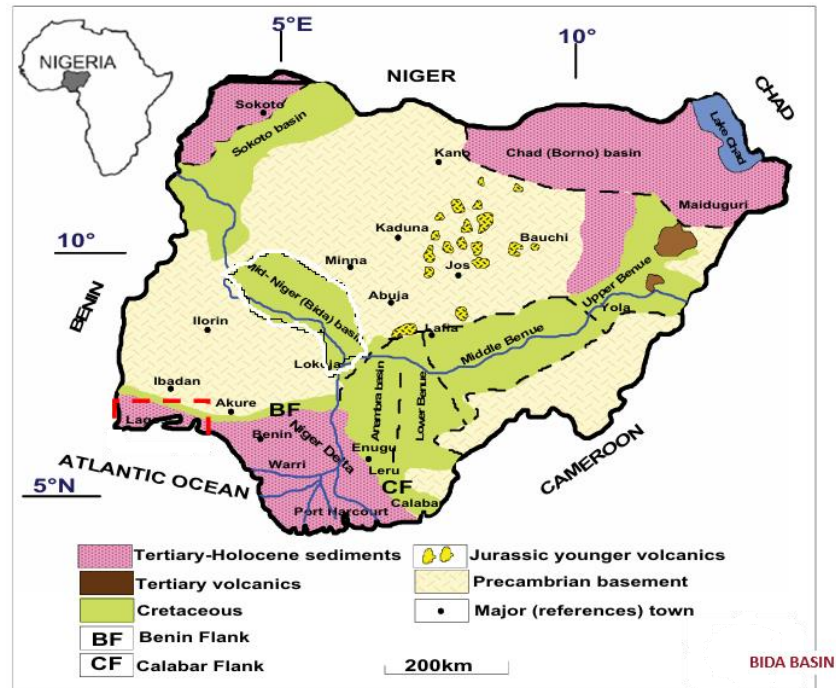


Fig. 1: Nigerian geological map of the research area (Modified After Obaje 2009)

1.1 Geology of the Study Area

According to Kande *et al.* (2005), there is a claim that the Anambra Basin flows into the Bida Basin from the northwest (Fig. 2). The sedimentary fill of the basin is composed of a band of Upper Cretaceous sedimentary rock strata that trends northwest and was formed because of block faulting, basement disintegration, and subsidence caused by the Cretaceous opening of the South Atlantic Ocean. The northern part is commonly referred to as the Bida sub-basin, while the southern portion is called the Lokoja sub-basin. The Bida Formation, which unconformably covers the Basement Complex, is in the basin's northern part. The basement is also unconformably covered by the Lokoja Formation, just like it is in the southern portion. The Bida and Lokoja Formations are juvenile in terms of texture and mineralogy. Conglomeratic sandstone, medium-grained sandstone, siltstone, and subordinate claystone are the finely aggregated products of massive conglomerates held up by a matrix and clasts (Ojo & Akande, 2013). Overlying the Lokoja Formation is the Patti Formation, which is made up of shale, sandstone, ironstone, and claystone. In the northern part of the basin, the Enagi Formation—a siltstone, sandstone, and claystone formation—lies atop the Bida Formation (Ojo 2020).

The Enagi and Patti Formations are directly covered by the Batati and Agbaja Formations, respectively, according to Adeleye (1974) and Akande *et al.* (2005). In addition to small amounts of ferruginous siltstone, claystone intercalations, and shale beds that have created near-shore shallow marine to freshwater fauna, the Batati Formation is made up of argillaceous, goethite, and oolitic ironstones (Adeleye, 1973). The Agbaja Formation is composed of oolitic and pisolitic ironstones, and its age is estimated to be Late Maastrichtian (Ojo *et al.*, 2020). The Bida Basin's structural characteristics are demonstrated by a system of NW-SE trending faults at its borders that connect to the surrounding crystalline basement topography. This fault system also suggests the basin's rift origin (Kogbe *et al.*, 1983; Rahaman *et al.*, 2018). There were no noteworthy lineaments, intrusions, or morphological characteristics within the sedimentary basin

(Salawu *et al.*, 2020). Conversely, one of the prominent structural characteristics of the underlying basement is the lateral continuity of the NNE-SSW trending Kalangai–Zungeru–Ifewara shear zones, which were created during the Pan-African orogeny (Salawu *et al.*, 2020).

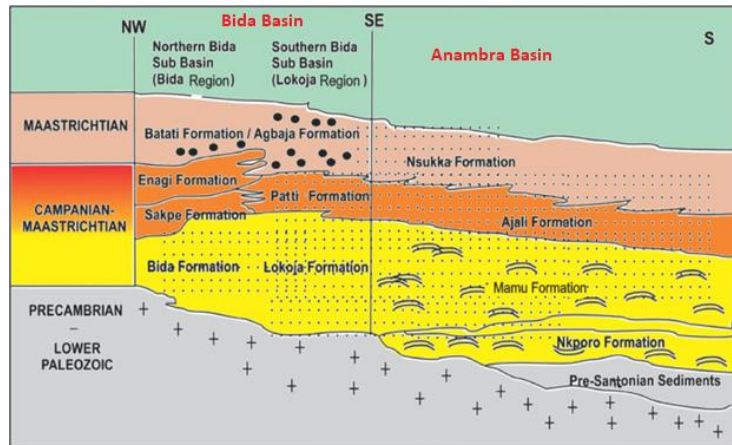


Fig. 2: Regional stratigraphic successions in the Bida Basin and NW-SE-S stratigraphic correlations from the Bida Basin to the Anambra Basin (Modified after Akande *et al.*, 2005)

2. Materials and Methods

2.1 Data acquisition

The Total Magnetic Intensity maps (TMI) on a 1:100,000 scale that were acquired during the Nigerian Geological Survey Agency's statewide aeromagnetic survey, which took place between 2005 and 2010, were employed in this study. The high-resolution aeromagnetic dataset, comprising sheets 182,183,184,203,204, and 205, for Mokwa, Egbako, Bida, Lafiagi, Pategi, and Baro respectively. NGSA (2010) states that data were collected and stored in a grid format at 100-meter sample intervals. In the NW-SE and NE-SW orientations, the travers and tie line spacings were 500 and 2000 meters, respectively. The study area is covered by six aeromagnetic maps of total field intensity on $\frac{1}{2}^\circ$ by $\frac{1}{2}^\circ$ sheets. The initial pre-processing of the data, which involved micro-leveling, removing cultural effects, and filtering for noise elements, was carried out by the Fugro Airborne Survey and Consultant teams. The pre-processed data were examined for anomalies and lone spikes unrelated to the geology. Any probable cultural noise and other absurd noise were removed using Butterworth filtering processing to maximize the signal-to-noise ratio and minimize other noise energy in the data. Maps of the region's total magnetic field intensity, including the sheets (Fig. 3), were created using the Oasis Montaj software.

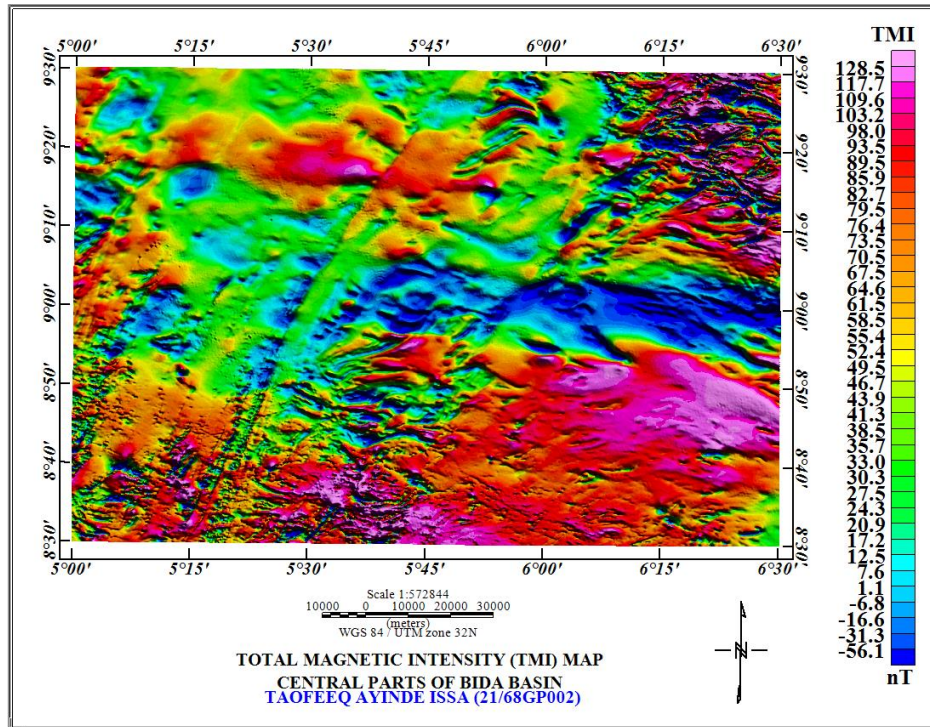


Fig. 3: Total Magnetic Intensity map of the research area.

2.2 Reduction to the Equator

The reduction involves correcting or adjusting the observed magnetic field components to what they would be if the measurements were taken at the magnetic equator. This is done by applying mathematical formulas that consider the latitude and inclination angle of the magnetic field at each measurement location, Fig. 4.

2.3 Regional – Residual Separation

Regional-residual separation is a technique used in geophysical data processing to distinguish between broad-scale (regional) and localized (residual) variations within a dataset. This separation is commonly applied to gravity and magnetic data but can also be used with other geophysical datasets. The goal is to isolate and enhance the signals associated with specific geological features or anomalies of interest, such as subsurface structures or mineral deposits.

2.4 Spectral Depth Analysis

Usually, measurements of the widths and slopes of individual anomalies in the aeromagnetic profiles are used to compute the spectral depths. This technique is based on the idea that magnetic signatures from all depths are integrated into a magnetic field that is detected at the surface. A function that varies continuously along an observation profile like the intensity of a magnetic field is transformed from the spatial domain to the frequency domain by the Fourier integral transform. The two-dimensional Fourier transform pair can be stated as follows in its complex form:

$$G(u, v) = \iint_{-\infty}^{\infty} g(x, y) e^{i(u_x - v_y)} d_x d_y \quad (1)$$

$$G(u, v) = \frac{1}{4\pi^2} \iint_{-\infty}^{\infty} g(u, v) e^{i(u_x - v_y)} d_u d_v \quad (2)$$

$$G(u, v) = P(u, v) + iQ(u, v) \quad (3)$$

The spectrum energy is expressed as follows,

$$E(u, v) = [G(u, v)]^2 = (P^2 + Q^2) \quad (4)$$

The energy spectrum expression in polar form by Spector and Grant, 1970 shows that if

$$r^2 = (u^2 + v^2) \text{ and } \theta = \arctan\left(\frac{u}{v}\right) \quad (5)$$

The energy spectrum $E(r, \theta)$ may well be assumed as:

$$(E(r, \theta)) = 4\pi^2 M^2 R_G^2 (e^{-2hr}) ((1 - e^{-tr})^2) (S^2(r, \theta)) (R_p^2(\theta)) \quad (6)$$

Estimation of the depth of magnetic field data is typically expressed according to

$$E(u, v) = \exp(-4\pi hr) \quad (7)$$

The power spectrum's dominating factor is the $\exp(-4\pi hr)$ phrase. The radial spectrum of the anomalous field is determined by calculating the average spectrum of the partial waves that fall within this frequency range. Should we swap out h for Z and r for f : then

$$\log E = -4\pi Zf \quad (8)$$

Here, Z represents depth, and f represents frequency. This transformed equation reflects how the power spectrum decays with depth and frequency, providing critical information for interpreting the subsurface magnetic sources. Therefore, the slope $m = -4\pi Z$ is obtained from the linear graph of a $\log E$ Versus f . The mean depth (Z) of the magnetic source is thus expressed by

$$Z = -\frac{m}{4\pi} = -m \times 0.08 \quad (9)$$

The procedures employed are as follows:

1. **Spectral block partitioning of the study area:** to help manage the massive quantity of data involved, the six residual grids of the study area were separated into 24 spectral blocks (BLK1-BLK24) (Figure 5).
2. **Generation of radial energy spectrum:** the residual magnetic data was converted into the radial energy spectrum for each block using Oasis Montaj.
3. **Plots of Ln of Power vs the frequency:** the source's depth determines the magnitude of the linear gradient present in its log-power spectrum. For each of the 24 spectral cells, graphs of spectral energy against frequencies were created. Bodies that occur within depth ranges are represented by points that lie on one or more straight-line segments. Shallow sources are represented by the line segment in the upper-frequency range, whilst deep-seated bodies are represented by the lower harmonics. A two-depth source model is revealed by the slopes of these graphs in the higher and lower frequency portions: Z_2 for deeper sources and Z_1 for shallower sources. In Figure 7, examples of these charts are displayed.

4. **Depth to magnetic sources estimation:** determination of the slopes of each line segment, then Equation (9) was used to estimate the mean depth (Z) of burial.

3. Results and Discussion

3.1. Result of Reduction to Magnetic Equator

Reducing the magnetic data to the Equator from Oasis Montaj software directly was not achievable as the method introduces drags at the edges of the anomalies, thus complicating the problem of symmetry which results from the dipolar nature of the magnetic data. The problem of drag results because the study area is closer to the equator than the pole. Hence, to achieve TMI reduced to the equator, the inverse of the values of IGRF corrected TMI reduced to the equator was computed and the result is shown in Figure 3 with the magnetic values ranging from -47.50 nT to 133.8 nT. The map shows that the area is dotted with several deep pockets of positive and negative anomalies. The basin's undulating morphology, which is mainly made up of magnetic ironstones nonmagnetic sandstones, and siltstones, may be the cause of these anomalies.

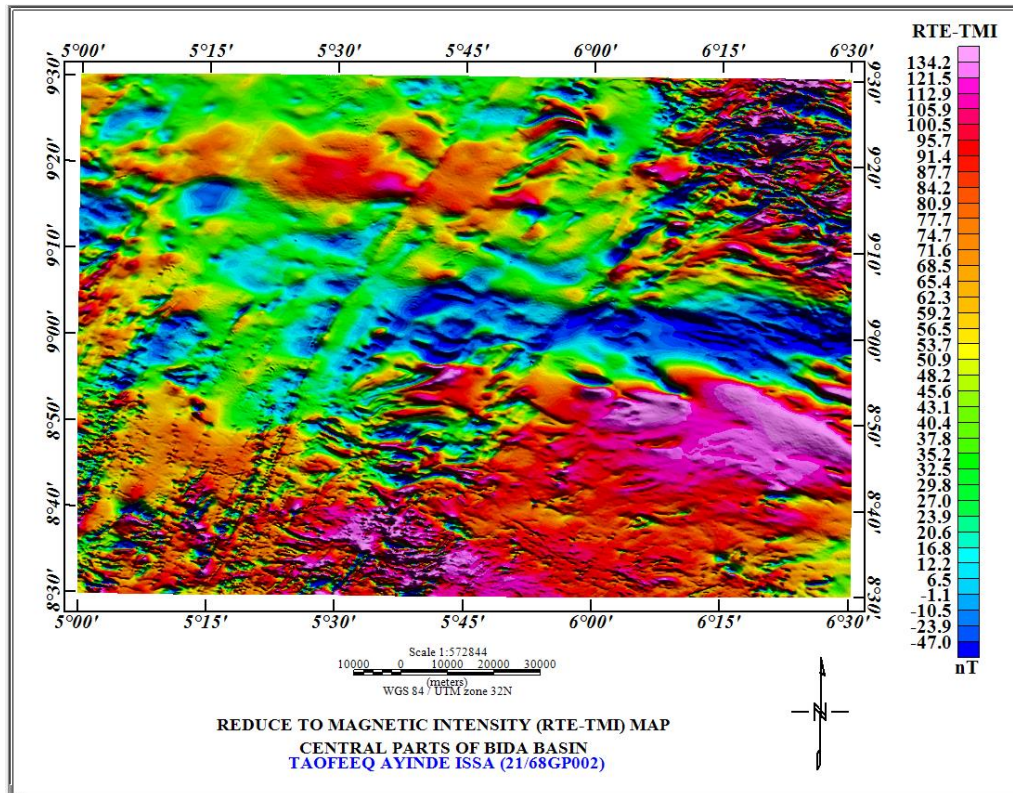


Figure 4: Reduce to Magnetic Equator map of the research area.

3.2 Results of Application of Spectral Depth Analysis

Spectral Depth Analysis was conducted on the residual magnetic data covering the entire area to determine the depth of basement rocks. The findings of the Spectral Depth Analysis are displayed in Fig. 5, which indicates that the average depth of 1.22 km is reached by the shallow magnetic sources, which range in depth from 0.68 km to 2.32 km. On the other hand, the average depth of the deeper magnetic sources is

3.26 km, ranging from 1.25 km to 5.88 km. Table 1 lists the locations for each of the twenty-four spectral blocks together with the two depth estimates (Z_1 and Z_2). The presence of near-surface magnetic sources, such as laterite, ironstones, or ferruginous sandstones, or a combination of two or more of these magnetic sources that intruded into the sedimentary section near the surface, could be the cause of the shallower magnetic sources. Additionally, there is a chance that the study area will be impacted by the magnetic basement that is adjacent. On the other hand, the presence of much deeper intrusions of the magnetic basement into the basin, lateral discontinuities in the basement, and other features within the study area with different magnetic properties, such as grabens, horsts, dykes, fractures, and faults could be responsible for the deeper magnetic anomalies. Fig. 6 is a representation of two of the spectral plots for blocks 15 and 23. Fig. 7 is the extrapolated map showing depths to deeper sources at a contour interval of 200 m. The graphs show laconically, areas with deep, moderate, and shallow depths to magnetic sources, with the deepest magnetic sources identified around the Egbako, represented by red color and bounded by latitudes $9.1^{\circ} N - 9.3^{\circ} N$ and longitudes $5.5^{\circ} E - 5.8^{\circ} E$. The areas shown in blue colors around Lafiagi, Pategi, and the northern part of the Bida block represent the depths of less deep magnetic sources.

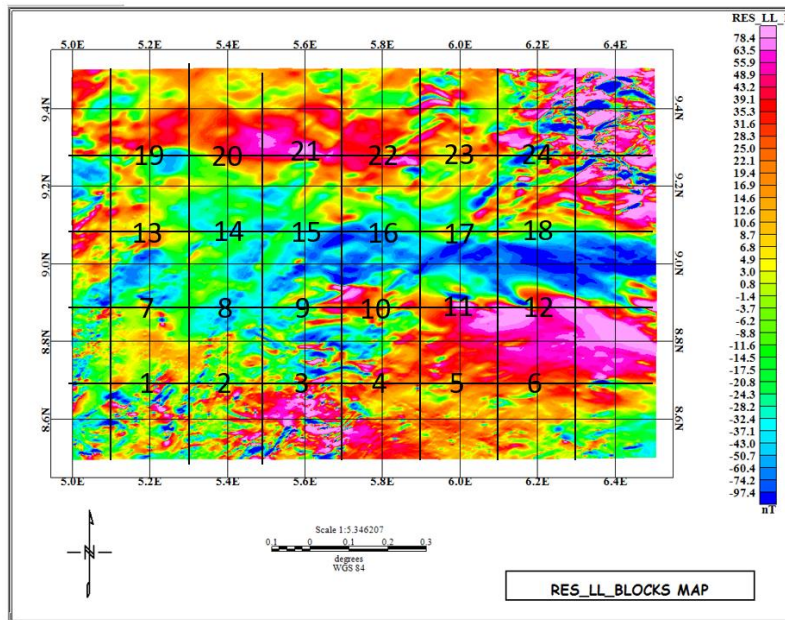


Fig. 5: The residual magnetic intensity from 1 to 24 separated into 24 overlapping square window blocks, each measuring 44 km by 44 km

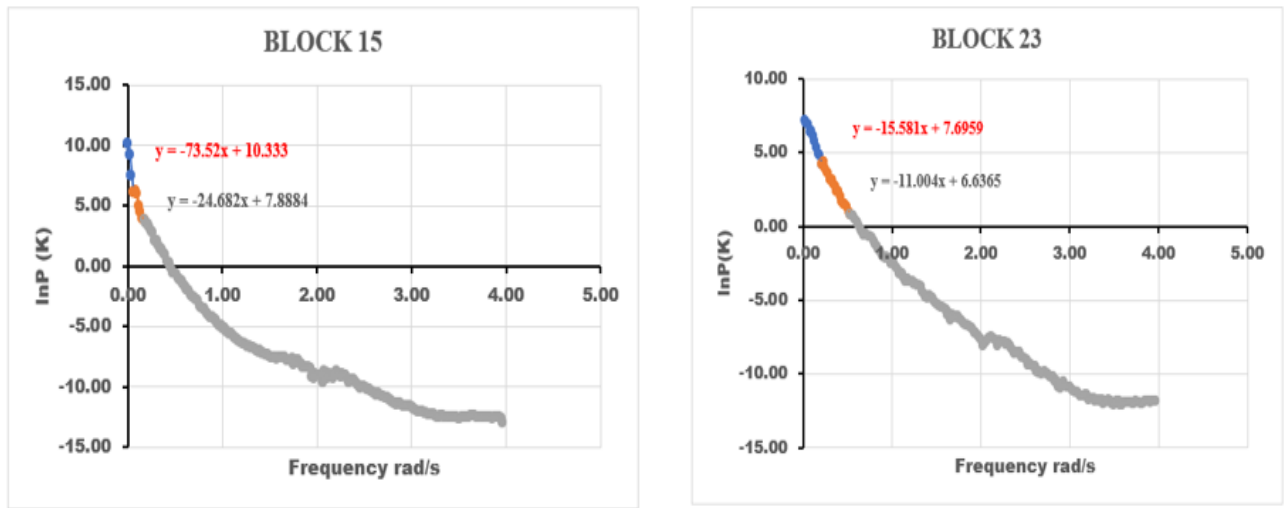


Fig. 6: The radial power spectrum for two blocks shows the following results: for block 15, the deeper slope (M_2) is 73.52 km, and the shallow slope (M_1) is 24.68 km, yielding a deeper source depth (Z_2) of 5.88 km ($0.08M_2$) and a shallow source depth (Z_1) of 1.97 km ($0.08M_1$). For block 23, the deeper slope (M_2) is 15.58 km, and the shallow slope (M_1) is 11.00 km, resulting in a deeper source depth (Z_2) of 1.25 km ($0.08M_2$) and a shallow source depth (Z_1) of 0.88 km ($0.08M_1$).

Table 1: Spectral depth of the 24 sets of magnetic sources, both deeper and shallower.

SN	BLOCKS	LONG -X ($^{\circ}$ E)	LAT -Y ($^{\circ}$ N)	M_2 (Km)	M_1 (Km)	Z_2 (Km)	Z_1 (Km)	BLOCK NAME
1	1	5.2	8.7	42.57	13.96	3.4056	1.1168	Lafiagi
2	2	5.4	8.7	33.00	10.63	2.6400	0.8504	Lafiagi
3	3	5.6	8.7	36.6	8.44	2.9280	0.6752	Pategi
4	4	5.8	8.7	26.94	10.71	2.1552	0.8568	Pategi
5	5	6.0	8.7	34.08	11.98	2.7264	0.9584	Baro
6	6	6.2	8.7	66.32	22.00	5.3056	1.7600	Baro
7	7	5.2	8.9	42.09	17.25	3.3672	1.3800	Lafiagi
8	8	5.4	8.9	19.47	11.98	1.5576	0.9584	Lafiagi
9	9	5.6	8.9	23.55	10.60	1.8840	0.8480	Pategi
10	10	5.8	8.9	28.70	11.38	2.2960	0.9104	Pategi
11	11	6.0	8.9	41.12	14.05	3.2896	1.1240	Baro
12	12	6.2	8.9	35.60	15.43	2.8480	1.2344	Baro
13	13	5.2	9.1	32.82	16.18	2.6256	1.2944	Mokwa
14	14	5.4	9.1	56.02	29.02	4.4816	2.3216	Mokwa
15	15	5.6	9.1	73.52	24.68	5.8816	1.9744	Egbako
16	16	5.8	9.1	55.49	22.64	4.4392	1.8112	Egbako
17	17	6.0	9.1	51.37	14.81	4.1096	1.1848	Bida
18	18	6.2	9.1	47.37	11.03	3.7896	0.8824	Bida
19	19	5.2	9.3	32.54	17.92	2.6032	1.4336	Mokwa
20	20	5.4	9.3	31.27	17.82	2.5016	1.4256	Mokwa

21	21	5.6	9.3	64.06	19.00	5.1248	1.5200	Egbako
22	22	5.8	9.3	65.48	13.25	5.2384	1.0600	Egbako
23	23	6.0	9.3	15.58	11.00	1.2464	0.8800	Bida
24	24	6.2	9.3	23.12	10.17	1.8496	0.8136	Bida
Minimum depth values (Km)						1.2464	0.6752	
Maximum depth values (Km)						5.8816	2.3216	
Total depth values (Km)						78.2944	29.2744	
Average depth values (Km)						3.262267	1.219767	

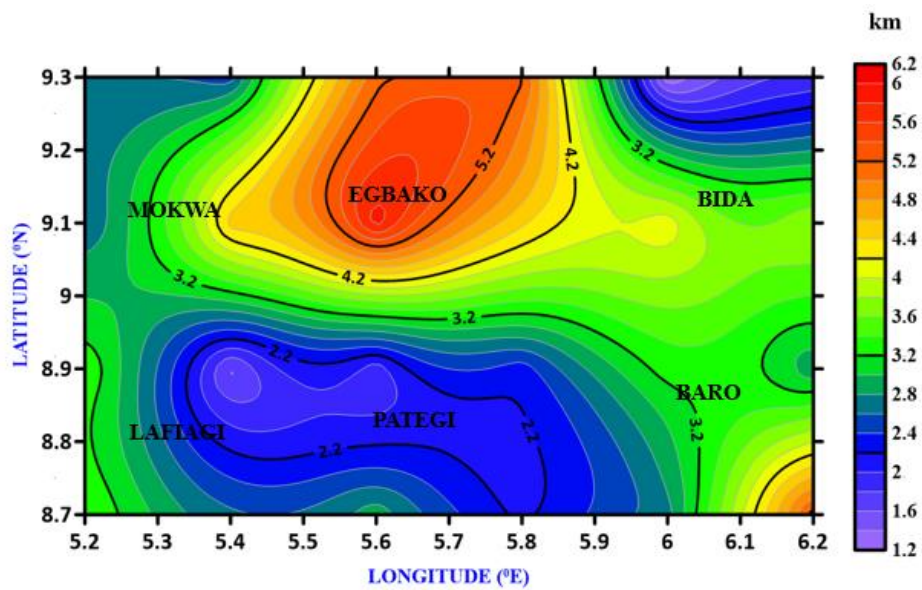


Fig. 7: Spectral Depth to a Deeper Source Extrapolation Map (Cont. Int. = 0.2 km)

Table 2: Showing the maximum and Minimum depths, deeper and shallow (Z2 and Z1) with locations

	MOKWA	Z2	Z1	EGBAKO	Z2	Z1	BIDA	Z2	Z1
Min		2.60	1.29		4.44	1.06		1.25	0.81
Max		4.48	2.32		5.88	1.97		4.11	1.18
	LAFIAGI	Z2	Z1	PATEGI	Z2	Z1	BARO	Z2	Z1
Min		1.56	0.96		1.88	0.68		2.73	0.96
Max		3.41	1.38		2.93	0.91		5.31	1.76

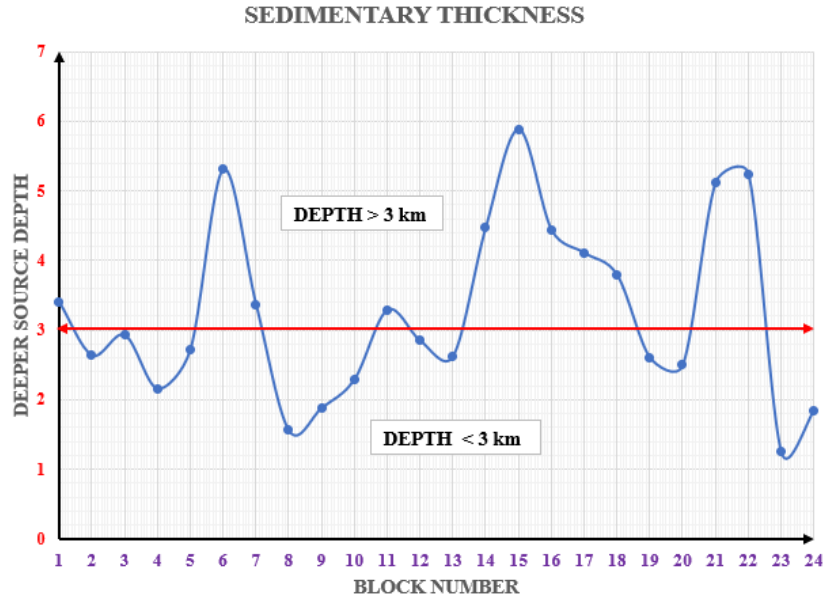


Fig. 8: Showing favorable depth for hydrocarbon generation

4. Conclusion

The research has effectively revealed the depths of the magnetic basement with the aid of the Spectral Depth Analysis method using aeromagnetic data from some areas around the Bida Basin of Nigeria. The application of Spectral Depth Analysis, revealed depths to the shallow magnetic sources (Z1) to range from 0.68 km on spectral block 3, which is the Pategi magnetic block to 2.32 km on the spectral block 14, Mokwa Block while the depth to the deeper magnetic sources, Z2, varies between a minimum of 1.25 km on the spectral block 23, Bida block and a maximum value of 5.88 km on spectral block 13 which lies on the Egbako block, with 45.83% of the blocks having depths above 3km (Table 2, Figure 8). Near-surface magnetic minerals, like laterite, ironstones, or ferruginous sandstones, could be connected to the shallower magnetic sources. These elements may have intruded into the sedimentary section near the surface, individually or in combination. Moreover, the study area's surrounding magnetic basement may have an impact on these shallow magnetic sources. On the other hand, the greater magnetic anomalies might result from far deeper penetrations of the magnetic basement into the basin. These anomalies may also be caused by lateral discontinuities in the basement and other geological features within the study area such as faults, fractures, dykes, grabens, and horsts that have varying magnetic susceptibilities. These results indicate that regions with sedimentary thickness values of more than 3 km, like blocks 1, 6, 7, 11, 14, 15, 16, 17, 18, 21, and 22 (Figure 8) should have their hydrocarbon potential further investigated.

Reference

- Adeleye, D. R. (1974). Sedimentology of the fluvial Bida Sandstones (Cretaceous) Nigeria. *Sedimentary Geology*, 12, 1-24. [http://dx.doi.org/10.1016/0037-0738\(74\)90013-X](http://dx.doi.org/10.1016/0037-0738(74)90013-X).
- Akande, S.O., Ojo, O.J., Erdtmann, B.D., Hetenyi, M, (2005). Paleoenvironments, organic petrology and Rock-Eval studies on source rock facies of the Lower Maastrichtian Patti Formation, Southern Bida Basin, Nigeria. *J. Afr. Earth Sci.* 41, 394–406.
- Kogbe, C. A. (1989). *Geology of Nigeria*. Rock View (Nigeria) Limited. Jos, Nigeria.

- Ojo, O.J., Akande, S.O., 2013. Petrographic facies, provenance, and paleoenvironments of the Lokoja Formation southern Bida basin, Nigeria. *J. Min. Geol.* 49 (2), 93–109.
- Ojo, O.J., Bamidele, T.E., Adepoju, S.A., Akande, S.O., (2020). Genesis and paleoenvironmental analysis of the ironstone facies of the Maastrichtian Patti Formation, Bida basin, Nigeria. *J. Afr. Earth Sci.* 174.
- Rahaman, M.A.O., Fadiya, S.L., Adekola, S.A., Coker, S.J., Bale, R.B., Olawoki, O.A., Omada, I.J., Obaje, N.G., Akinsanpe, O.T., Ojo, G.A., Akande, W.G., (2018). A revised stratigraphy of the Bida Basin, Nigeria. *J. Afr. Earth Sci.*
- Salawu, N.B., Fatoba, J.O., Adebisi, L.S., Ajadi, J., Saleh, A., Dada, S.S., (2020). Aeromagnetic and remote sensing evidence for the structural framework of the middle Niger and Sokoto basins, Nigeria *Phys. Earth Planet. In.* 309.
- Spector, A., and Grant, F.S. (1970), *Statistical Models for interpreting aeromagnetic data.* *Geophysics* Vol. (35), 293-302.